

# DISCRETE MOLECULAR DYNAMICS SIMULATION OF HARD REGULAR TRIANGLES

SCOTT CARMICHAEL

CHE 210D: MOLECULAR SIMULATION

*Department of Chemical Engineering*

*University of California, Santa Barbara*

June 15, 2012

## Abstract

Perhaps the most paramount utility of a ‘toy model’ simulation is its ability to shed light on the fundamental driving forces behind seemingly complex phenomena such as self-assembly, order-disorder phase transitions, and the nature of symmetry breaking. Recent experimental work reported by the Mason group has revealed that the ostensibly mundane system of hard triangles colliding on a 2-dimensional surface, in fact exhibits a rich array of order-disorder phase transitions and intriguingly local chiral symmetry breaking [Zhao, Kun, Robijn Bruinsma, and Thomas G. Mason.; Nat Commun 3 (May 2012): 801]. Here we use discrete molecular dynamics to simulate a system of hard regular triangles undergoing elastic Newtonian collisions on a 2-dimensional surface. We observe a disorder to order phase transition at packing fractions above 0.56, and we calculate the mean-squared displacement of triangles in the liquid-like regime.

## I. INTRODUCTION

While regular triangles are completely achiral as monomers, they are chiral as 'slightly off-set' dimers (see Figure 1). The Mason<sup>1</sup> group recently discovered that dense systems of such triangles on a flat surface will spontaneously break symmetry, and form domains where all dimers are one chiral form or the other. Further, the group measured the mean squared displacement vs. time of triangles at different packing fractions (e.g., area of the triangles / total area). They found that the systems remained slightly diffusive even at high packing fractions (where individual triangles are confined to cages), and attributed this affect to the collective transport of triangles along allowable slip directions. These intriguing results should be observable through a computer simulation.

Here we employ discrete molecular dynamics to simulate hard triangles on a 2-d surface, at a variety of packing fractions. Discrete molecular dynamics uses discontinuous 'hard wall' interactions between particles, and as such allows for distinct collision events to occur where the angular and linear momentum of two particles are exchanged through an impulse according to newton's equations of motion. This is quite different than conventional molecular dynamics where the interactions potentials are continuous, and collision events are spread out over some finite time interval. Because of the existence of distinct collision events in discrete molecular dynamics, it is possible to step the system from collision to collision, solving for the new momenta at each step, and thus avoid the highly discretized numerical integration inherent to conventional molecular dynamics.

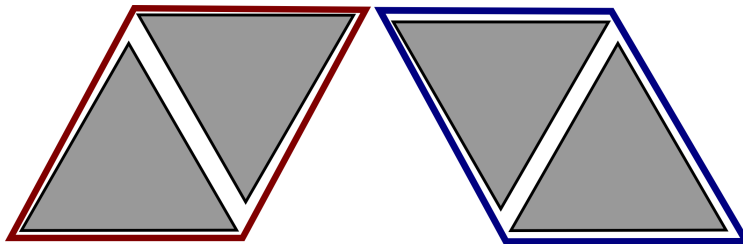
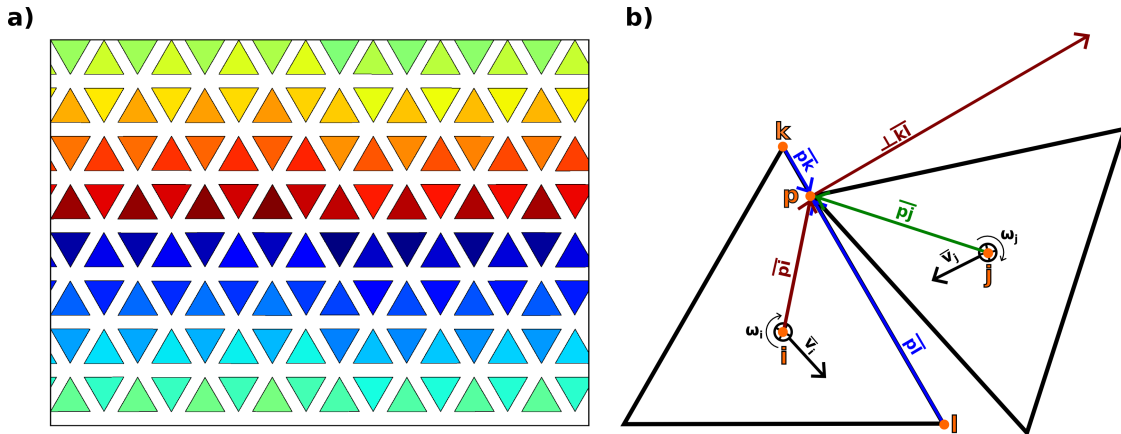


FIG. 1: The two enantiomers of triangle dimers.

## II. METHODS

A system of regular triangles is initialized on a hexagonal lattice with an interparticle spacing consistent with a target packing fraction (see Figure 2a). The initial linear and



**FIG. 2:** (a) An initial configuration of triangles at a packing fraction  $\Phi = 0.42$ , triangles colored by row index. (b) A schematic of a collision event, with the vectors that are relevant to the collision detection and resolution algorithm (described below) labeled.

angular velocities of each triangle are assigned from a normal random distribution. The system is then stepped forward through time, and if a collision is detected an exchange in momenta is applied and the system continues on through time. At the heart of this process is the collision detection and resolution algorithm.

### A. Collision Detection and Resolution

Neighbor lists are created at each time step, and every pair of neighbors are tested for overlap. The overlap detection routine performs a simple line cross test for every combination of chords for the triangles in question. If an overlap is detected, then the point of impact is determined, and the new momenta resolved. Figure 2b shows a schematic of a typical collision, and defines various vectors that are employed by the algorithm to detect and resolve collisions. The algorithm uses a hierarchy of tests to determine the point of impact in both time and space. In general, it tests each vertex 'p' on an impinging triangle (triangle j in Figure 2b) for collinearity with each chord 'kl' of a target triangle. A dot product is employed for this test and is given by,

$$\vec{pk} \cdot \perp \vec{kl} \approx 0 \quad (1)$$

where the vectors reference those found in Figure 2b. If a point is found to be collinear with a chord, it is then determined if the point actually lies on the chord using,

$$|p\vec{k}| + |p\vec{l}| \approx |k\vec{l}| = 1 \quad (2)$$

where  $k\vec{l}$  has a magnitude of 1 by design. If point ‘p’ lies on the chord ‘kl’ then it is necessary to determine if the two are converging towards one another (as in a impending collision) or if they are diverging (as is the case immediately following a collision). This test is achieved by looking at the sign of the relative velocity of the point and the chord as projected on the the vector normal to the chord, e.g.,

$$v^{\vec{p}}_{ij} \cdot \perp k\vec{l} \leq 0 \quad (3)$$

where the relative velocity is given by,

$$v^{\vec{p}}_{ij} = (\vec{v}_i + \perp p\vec{i} \times \omega_i) - (\vec{v}_j + \perp p\vec{j} \times \omega_j). \quad (4)$$

Now, if the point and the chord are converging then the collision time can be found using,

$$t = \frac{p\vec{k} \cdot \perp k\vec{l}}{v^{\vec{p}}_{ij}}. \quad (5)$$

In practice, a small error in the collision time is introduced here, because point ‘p’ is actually traveling along a cycloid and not a straight line. A refined collision time is determined by iteratively stepping to the estimated collision time and calculating a new updated collision time. This procedure converges onto the true collision time (to within six significant figures) within 3 iterations. For each time step, the collision time for all overlapping triangles is calculated and the system is evolved to the first collision. At this point all that is left to resolve is the post collision momenta of the triangles. The collision impulse is given by,

$$I = \frac{-2v^{\vec{p}}_{ij} \cdot \perp k\vec{l}}{2 + (\perp p\vec{i} \cdot \perp k\vec{l})^2 + (\perp p\vec{j} \cdot \perp k\vec{l})^2}. \quad (6)$$

This impulse is then applied to the linear and angular velocities of triangle  $i$ ,

$$\vec{v}'_i = \vec{v}_i + I \times \perp \vec{k}l \quad (7)$$

$$\omega'_i = \omega_i + \perp \vec{p}i \cdot I \vec{k}l \quad (8)$$

and similarly for the momenta of triangle  $j$  (although the impulse is reversed).

### III. RESULTS

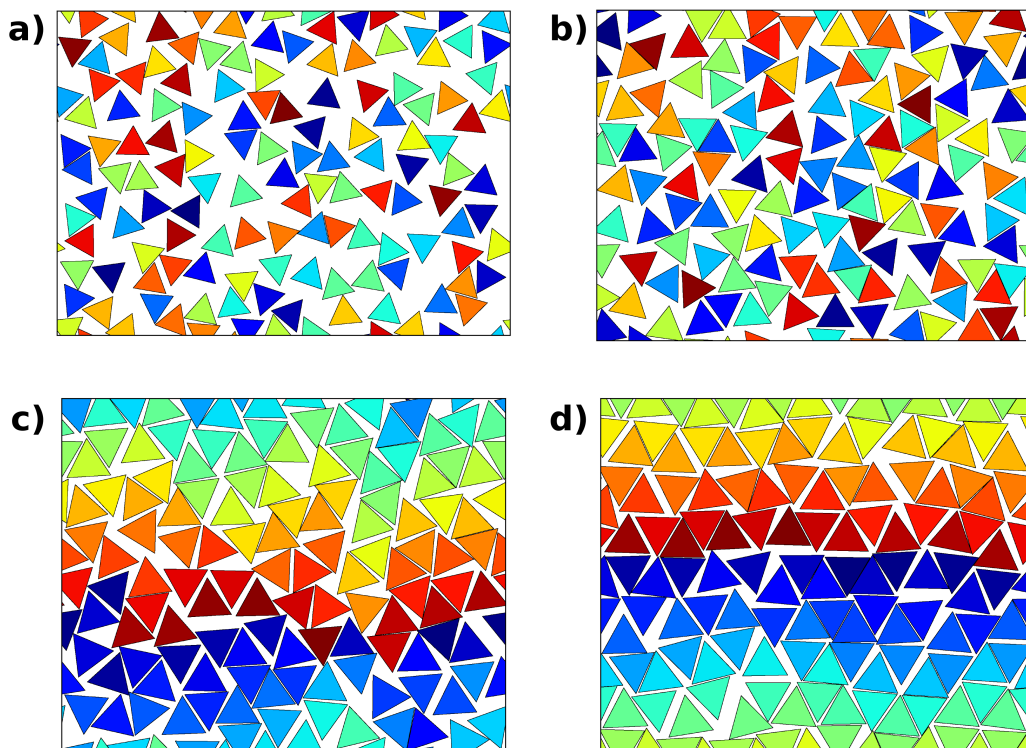


**FIG. 3:** Simulation snapshots taken at different packing fractions. (a)  $\Phi = 0.42$  (b)  $\Phi = 0.56$  (c)  $\Phi = 0.69$  (d)  $\Phi = 0.74$

Simulations were performed for packing fractions  $\Phi = 0.42, 0.56, 0.69, 0.74, 0.80, 0.90$  and the mean-squared displacement (MSD) vs. time was plotted for systems that exhibited significant drift. Representative snapshots of these systems are found in Figure 3. Notably, we did not observe the local chiral symmetry breaking (at packing fractions above 0.69) that was found in the experiment by the Mason group. This is likely due to the absence of Brownian forces in these simulations. We do however see the order-disorder phase transitions.

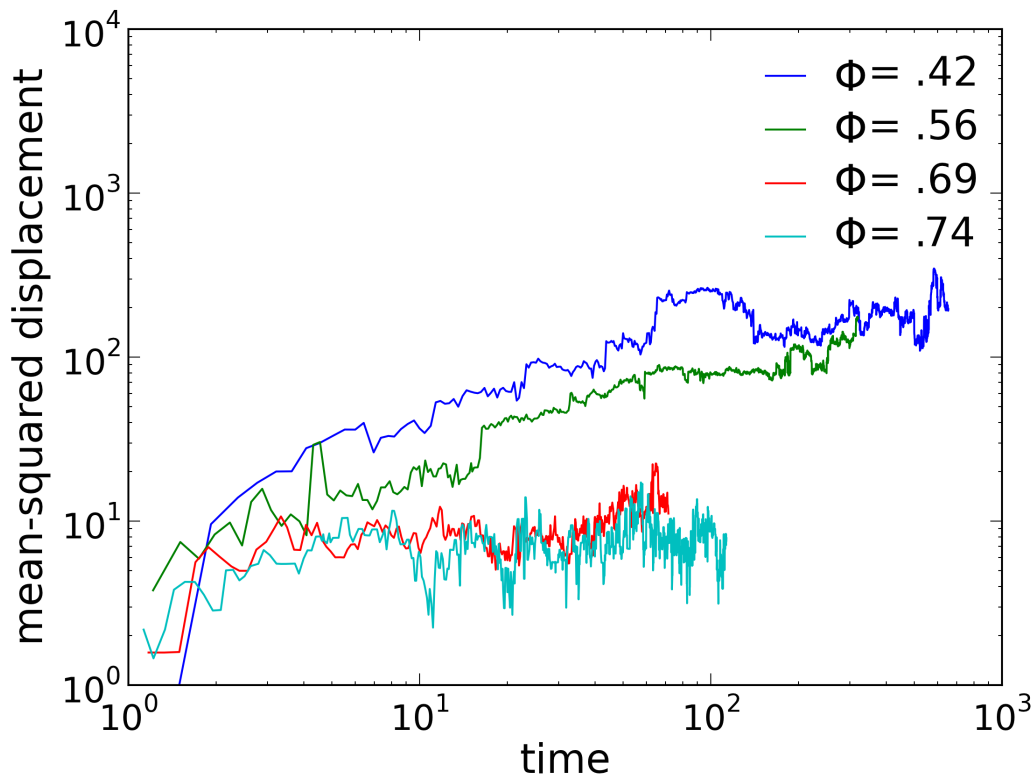


**FIG. 4:** The mean-squared displacement of particles systems at various packing fractions.

At packing fractions below 0.69, the system is disordered, while at higher packing fractions significant ordering is observed. As seen in Figure 4, low packing fraction systems exhibit substantial drift (in the diffusive regime), while the denser, more ordered systems, have only random local drift. This result contradicts the experimental finding of drift even at relatively high packing fractions. This discrepancy can be attributed to the lack of Brownian forces in the simulation, because as Mason points out “Thermal fluctuations can drive collective translational motion of many triangles in concert...”. So in the absence of thermal forces, there is no driving force for collective motion.

It should be noted that these data are taken from a limited sample size, and given more time, much better resolved MSD plots could be obtained. Further, Brownian motion could be incorporated into this model via the addition of ‘thermal kicks’ to randomly chosen triangles, in a method analogous to the Andersen thermostat.

#### IV. CONCLUSION

We have developed a discrete molecular dynamics simulation to study the ordering of regular triangles on a 2-dimensional surface. A robust collision detection and resolution routine was required to accurately resolve the Newtonian dynamics. We failed to recapitulate experimental finding of local chiral symmetry breaking in such systems as reported by Mason and co-workers, and we hypothesize that the lack of Brownian forces in our model precluded this. We did, however, observe a disorder-order phase transition above a packing fraction of 0.56.

#### V. REFERENCES

1. Zhao, Kun, Robijn Bruinsma, and Thomas G. Mason. Local Chiral Symmetry Breaking in Triatic Liquid Crystals. *Nat Commun* 3 (May 1, 2012): 801.